

Modeling non-planar coils in a full-scale stellarator

M. Backmeyer, N. Riva, M. Lyly, A. Halbach, and V. Lahtinen

Abstract—Design and modeling of a stellarator fusion reactor is a multidisciplinary effort that requires a tight integration between simulation of highly nonlinear multi-physics and representation of non-planar complex geometries. The critical current calculation and the design of the mechanical structures are among the most crucial aspects as they set size, cost, and time to build the stellarator. Because of the asymmetric and non-planar nature of its components the modeling of such figures of merit needs to be carried out at large scale, without the possibility of taking advantage of any particular symmetry. In this work we develop a three-dimensional model for the analysis of the magnetic field and forces, necessary for such considerations, for complex coil geometries, such as stellarators, where a two-dimensional approach can not provide accurate analyses and verification of assumptions. Moreover, this method can quickly generate a large amount of critical modeling data (e.g. Lorentz load, displacement and stresses) that could be integrated into a workflow for coil design optimization based on machine learning or other recent optimization tools.

Index Terms—fusion, stellarator, simulation, DDM, non-planar geometry

I. INTRODUCTION

THE most advanced approach for nuclear fusion involves using toroidal magnetic confinement systems, specifically Tokamaks and Stellarators. Both systems use magnetic fields to confine the plasma. In both Tokamaks and Stellarators, particles can drift off course and hit the chamber walls due to the inhomogeneous magnetic field. In Tokamaks one set of coils generates a toroidal field, a central solenoid operated in pulsed mode induces a toroidal current in the plasma, and a third set of coils generates an outer poloidal field that shapes and positions the plasma. The combination of the field components result in a twisted magnetic field that confines the particles in the plasma. Stellarators confine the plasma by means of non-planar coils only, eliminating the need for the solenoid/transformer. This allows Stellarators to operate without plasma disruption (typically problematic for Tokamaks) and in a steady state for continuous energy production [1], [2]. For the stellarator coil optimization in the design process, it is crucial to have an accurate simulation of the magnetic field and loads on the coils to meet physics requirements and engineering constraints. Therefore, Finite Element Modeling (FEM) tools are mandatory to analyze the

electro-magneto-thermal and mechanical response of a high-temperature superconductor (HTS) non-planar coil [3] and predict its safe-operation behavior. Even with an accurate knowledge of the coil geometry, it is challenging to predict its performance accurately. Not only too large Lorentz loads can damage the tape and reduce the coil’s performance [4], but excessive deformation of the coil systems can lead to a poor performance of the plasma confinement itself [5]. The non-planarity of stellarator coils, may require to solve full scale three-dimensional (3D) FEM problems with much larger number of degrees of freedom with respect to Tokamaks due to the absence of trivial symmetries (such as the axisymmetric one in tokamaks) [6]. The computational limit with sequential computing or even loop-level parallelism is quickly reached. In this work we present the analysis of the magnetic field and Lorentz loads of a full-scale stellarator based on the Helias-3 configuration [7], [8] using the domain-decomposition methods (DDM) which leads to short computation times and high accuracy. This is a continuation of our previous work, where we introduced `Quanscient Allsolve`, a custom cloud-based simulation tool in the context of DDM-accelerated quench and AC loss simulations [9].

Computational times of large and complex FEM scale models in the order of minutes could enable the use of Artificial Intelligence (AI) tools to corroborate and perform generative design to optimize the mechanical structures.

In section II we describe the procedure to obtain the coil orientations, briefly mention the formulation and describe the utilized custom DDM tool. In section III, we present our results, compared to results using `COMSOL`, and a mesh sensitivity study. Finally, in section III we draw conclusions.

II. COMPUTATION MODEL

The stellarator geometry that will be analyzed is shown in Figure 1 and is based on the HELIAS-3 [7], [8]. This configuration consists of 30 coils and produces an average magnetic field on the magnetic axis (the “middle line” of the plasma in Fig 1) of 8.9 T. The theoretical value is calculated using the Biot-Savart law. One of the purposes of this work is to evaluate the Lorentz loads on the coils and use this as an input (for future works) to design the mechanical radial plates. Simulating in high-detail (full-turns) all the coils is impractical and unnecessary. A possible approach is to focus on the mechanical design of a single coil (See Figure 1 inset) and simulate the overall magnetic field experienced by that coil (self-field + remaining coils) where $N_{\text{coil}} - 1$ coils are homogenized (all the turns are considered to be homogenized in one single turn) and the single coil of interest is simulated in great detail. This approach allows to focus on one coil at the time and generate data (i.e. Lorentz loads) for a reduced

M. Backmeyer, M. Lyly, A. Halbach, and V. Lahtinen are with Quanscient Oy (Tampere, Finland) (e-mail: merle.backmeyer@quanscient.com, mika.lyly@quanscient.com, alexandre.halbach@quanscient.com, valtteri.lahtinen@quanscient.com)

N. Riva is with MIT Plasma Science and Fusion Center (MA, USA) (e-mail: nicoriva@mit.edu)

This work was supported by Quanscient and by CFS and PSFC-MIT via RPP27. We want to thank Jorrit Lion (jlion@proximafusion.com) for providing the geometry of the stellarator.

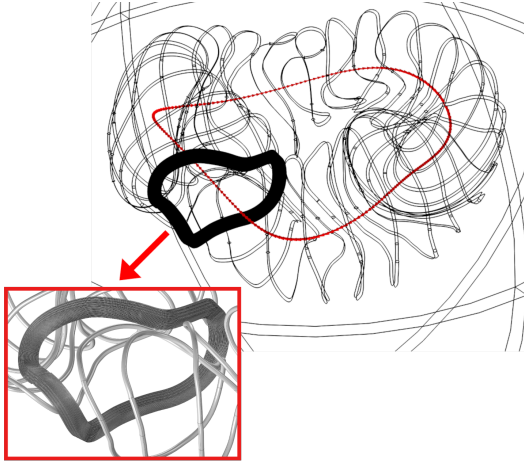


Fig. 1. The geometry of the full stellarator with a diameter of approx. 20 m.

and separate model (3D mechanical) that can be used for coil design in an optimization workflow.

Specifically, in this work the stellarator is composed of a total of 30 non-planar coils: 29 coils are homogenized with rectangular cross-section and carry 13.27 MA; one of the coils only is modeled on a detailed level with 208 turns (see Figure 1 inset) and carries $I_{op} = 63\,798$ A (i.e. 13.27 MA/208). A magnetostatic field map study of the full-stellarator assembly is carried out by applying the current density to each of the 29 homogenized coil as well as to the 208 turns of the detailed coil (see section II-A). Note that given the complex geometry of each coil, it's necessary to determine local curvilinear coordinates aligned with the coil/turn orientations via numerical method similar to the methods utilized in [3], [10] to introduce the current density normal to each coil. In these works the utilized software was COMSOL, where a Curvilinear Coordinate module (or the Coil Geometry Analysis) can be used for this purpose. In this work we introduce a new method based on the Laplace equations (see section II-B).

Finally, solving the problem was accelerated using Domain Decomposition Method (DDM) on an Amazon Web Services (AWS) cloud infrastructure suited for multiphysics DDM, provided by Quanscient (www.quanscient.com) under the Quanscient Allsolve software. Its distributed memory management ensures memory requirements will not be a bottleneck.

A. Magnetostatic A Formulation

The computational domain Ω consists of air Ω_{air} and conducting coils Ω_{coil} and is enclosed by the domain boundary $\partial\Omega$. The well-known A-formulation is solved to find the distribution of the the magnetic vector potential \mathbf{A} . The discretization of the magnetic vector potential A is carried out using Whitney edge elements [11].

B. Curvilinear Coordinates

To introduce the current density \mathbf{J} oriented along the cable, the curvilinear coordinates of the cables/turns need to be

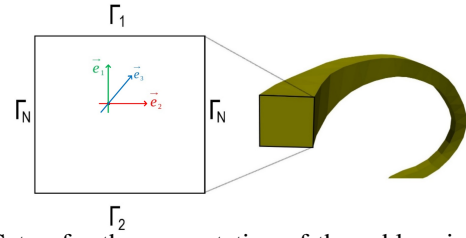


Fig. 2. Setup for the computation of the cable orientation.

determined. A local coordinate system is introduced at each point in the cable (see Figure 2) and described by the gradients of the three scalar potentials φ_1 , φ_2 and φ_3 , i.e.

$$\vec{e}_1 = \nabla\varphi_1, \vec{e}_2 = \nabla\varphi_2, \vec{e}_3 = \nabla\varphi_3. \quad (1)$$

Exploiting the mutual orthogonality of the surfaces Γ_1 and Γ_2 , the scalar potential φ_1 is obtained solving a Laplace problem. It represents the solution to the boundary value problem,

$$\Delta\varphi_1 = 0 \text{ on } \Omega \quad (2)$$

$$\varphi_1 = 0 \text{ on } \Gamma_1 \quad (3)$$

$$\varphi_1 = 1 \text{ on } \Gamma_2 \quad (4)$$

$$\mathbf{n} \cdot \nabla\varphi_1 = 0 \text{ on } \Gamma_N. \quad (5)$$

Repeating this procedure for φ_2 with interchanged boundary conditions

$$\varphi_2 = \begin{cases} 0 & \text{on } \Gamma_N \\ 1 & \text{on } \Gamma_1 \end{cases} \quad (6)$$

$$\mathbf{n} \cdot \nabla\varphi_2 = 0 \text{ on } \Gamma_1 \text{ and } \Gamma_2, \quad (7)$$

we get with $\nabla\varphi_1$ and $\nabla\varphi_2$ two base unit vectors of the local curvilinear coordinate system at any point of the coil. The cross product of $\nabla\varphi_1$ and $\nabla\varphi_2$ defines the third basis vector of the coordinate system, which is orthogonal to the cross section and represents the direction of the current flow $\frac{\mathbf{J}}{\|\mathbf{J}\|}$, so

$$\nabla\varphi_1 \times \nabla\varphi_2 = \frac{\mathbf{J}}{\|\mathbf{J}\|}. \quad (8)$$

Figure 3 shows the intermediate steps of the methods on one exemplary coil. This approach can also be used to model the dependency of the critical current on the magnetic field orientation. In that case, it is used to determine the perpendicular and parallel field components for any tape orientation.

C. Domain Decomposition Method

The domain decomposition method (DDM) in the FEM context refers to the partitioning of the computational mesh into similarly sized pieces that can each be processed on different computing instances, allowing to distribute the computational burden. The DDM method is used to improve the speed of numerical simulations in solid mechanics, electromagnetism, flow in porous media, etc., on parallel machines from tens to hundreds of thousands of cores. This is well suited to take advantage of supercomputer or cloud architectures, which was

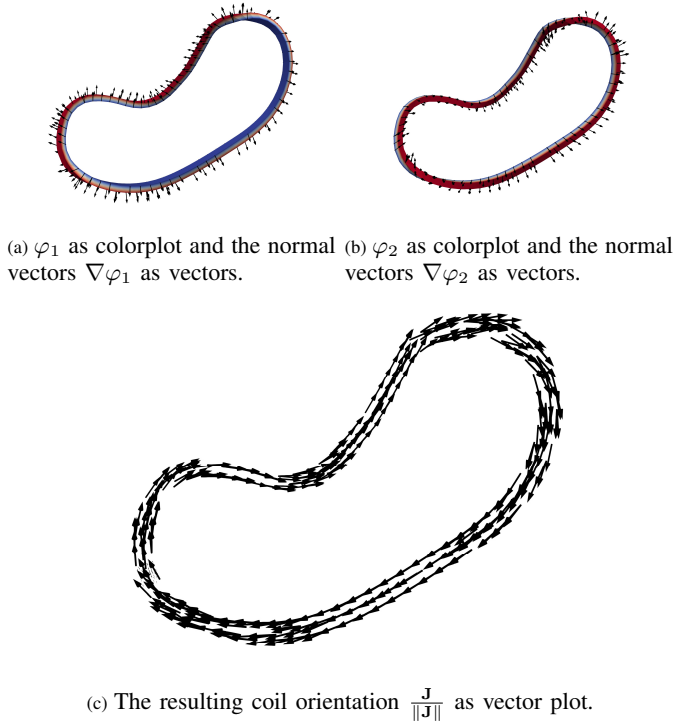


Fig. 3. Intermediate steps to find the orientations of the coils/turns.

already shown in [9]. In this work, the optimized Schwarz algorithm is used in the DDM framework: this algorithm solves the problems defined on the smaller mesh pieces iteratively using generalized minimal residual method (GMRES) and exchanges boundary data between domains at each iteration to reach convergence. Compared to the pioneering work of [12] the method used in this work accelerates convergence using GMRES and optimized boundary data [13].

III. RESULTS

A. Field plots

The numerical study is conducted for different interpolation orders and mesh resolutions. First of all, the resulting fields for the coarser mesh and cubic elements are presented. In Figure 4, the distribution of the magnetic field in the full stellarator is shown. It matches well the expected theoretical value of 8.9 T on the magnetic axis.

Figure 5 depicts the magnetic field map on the cable volume, and its peak is 15.45 T. If we consider an $I_{op} = 63\,798$ A and a $B_{peak} = 15.45$ T we expect a peak of the Lorentz load of $F_{dens} = I \times B \simeq 980$ kN·m⁻¹. Figure 6 represents the Lorentz force density defined as $I \times B$ that could be used as an input for a mechanical model to evaluate what are the maximum stresses experienced by the coil. The maximum of the Lorentz load of 0.975 MN·m⁻¹ is in reasonable agreement with the rough calculation estimated above and with the maximum Lorentz loads in literature [14]–[17].

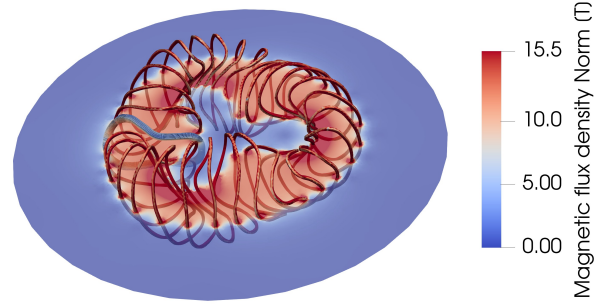


Fig. 4. Magnetic flux density of the full-scale stellarator.

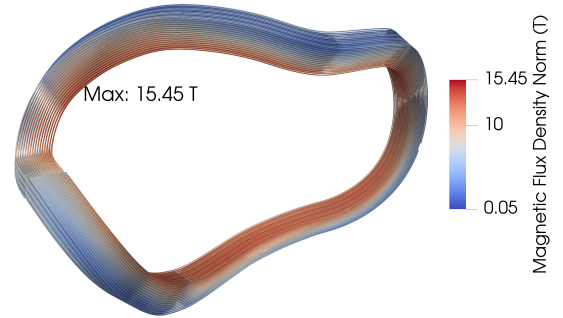


Fig. 5. Magnetic field B on the full-scale full-turns detailed coil.

B. Validation against COMSOL Multiphysics

The solution was validated against another simulation software, namely the commercial software COMSOL Multiphysics [18], in which a direct solver for the coil analysis, and an iterative solver with Auxiliary-Space Maxwell (AMS) preconditioner for the magnetic problem were used. In both simulation tools, the discretization was performed using linear elements. Figure 7 shows the comparison of the magnitude of the magnetic flux density on the magnetic axis (marked in red in Figure 1) obtained from both simulations of the stellarator. The different coil orientation acquisition methods (Coil Geometry Analysis vs. Laplace Problem) lead to computations on distinct mesh configurations. The analysis with COMSOL was performed on coils represented with circu-

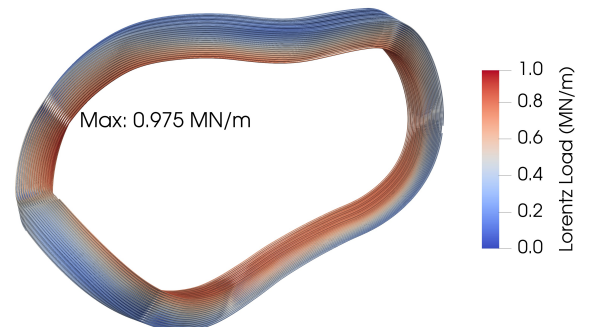


Fig. 6. Lorentz loads on the full-scale full-turns detailed coil.

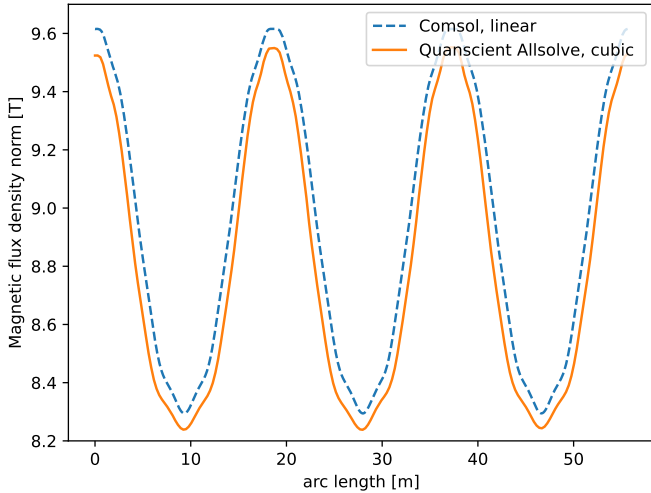


Fig. 7. Comparison of the magnetic field flux along magnetic axis between COMSOL (dashed) and Quanscient.allsolve (continuous).

lar cross sections. That explains the slight mismatch of 0.66 % of the peak values.

The runtime statistics of both simulations will be compared in subsection III-D.

C. Mesh sensitivity analysis

As a next step, we study the dependency of the solution on the mesh resolution and the interpolation order. The same simulation was repeated for a finer mesh, obtained by splitting the elements, and for linear and cubic interpolation order. Results are presented in Figure 8. Increasing the interpolation order leads to smoother field results. The solutions of the two mesh resolutions for cubic interpolation differ by a RMSE below 0.8%, indicating that all effects are already covered by the coarser mesh. However, the ability to perform large simulations on different mesh resolutions enables the use of machine learning models for (mechanical) optimization. Multi-level machine learning algorithms learn on the differences of the observable on successive mesh resolutions [19].

D. Runtime statistics

Table I states the number of unknowns, the number of cores used and the computation time for different model setups. The advantage of using DDM is clearly visible if we compare the different simulations that were run on Quanscient Allsolve. For example, an increase of the number of DoFs by around 8 (see column 2 and 3) has rarely any effect on the runtime if the number of cores is adapted as well. Using DDM with Quanscient Allsolve makes it even possible to run the largest problem of over 317 million DoFs in 17 minutes.

IV. CONCLUSION

In this paper, a magnetostatic simulation of a full-scale stellarator was carried out. Utilizing Quanscient Allsolve, an in-house Domain Decomposition Method (DDM) tool was

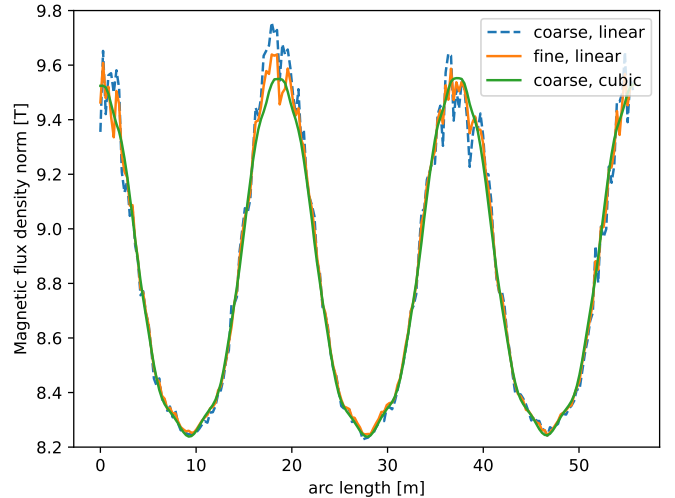


Fig. 8. Magnetic flux density norm on axis of the stellarator compared for different orders and mesh resolutions.

TABLE I: Comparison of the computation times for different setups.

Software	COMSOL	Quanscient Allsolve	Quanscient Allsolve	Quanscient Allsolve
Shape function order	linear	linear	cubic	cubic
Mesh resolution	coarse	coarse	coarse	fine
MDoFs	1.5	5	39	317
Computer	16 cores, 96 GB RAM	15 Cores	50 Cores	500 Cores x 2 CPUs
Runtime (min)	23	< 4	4	17

benchmarked against COMSOL, while also demonstrating better scalability on cloud infrastructure. In addition, the Laplace problem was solved to individuate the correct current flow along the complex path of the stellarator coils.

A single coil was modeled in high detail, while homogenizing the others. This allowed us to capture the magnetic field and, consequently, Lorentz loads experienced by the chosen coil, considering both its self-field and contributions from the remaining coils.

The results, when compared with those obtained from COMSOL, showcased a high degree of accuracy. Furthermore, a mesh sensitivity analysis showed the advantages of higher interpolation orders over finer mesh refinements.

Ultimately, this method serves as a stepping stone to rapidly generate large amount of critical data such as Lorentz loads, displacement, and stresses. These data can be integrated into a workflow for coil design optimization, potentially leveraging machine learning or other contemporary tools.

REFERENCES

- [1] T. S. Pedersen, M. Otte, S. Lazerson, P. Helander, S. Bozhnikov, C. Biedermann, T. Klinger, R. C. Wolf, and H.-S. Bosch, "Confirmation of the topology of the wendelstein 7-x magnetic field to better than 1: 100,000," *Nature communications*, vol. 7, no. 1, p. 13493, 2016.
- [2] T. S. Pedersen, R. König, M. Krychowiak, M. Jakubowski, J. Baldzuhn, S. Bozhnikov, G. Fuchert, A. Langenberg, H. Niemann, D. Zhang et al., "First results from divertor operation in wendelstein 7-x," *Plasma Physics and Controlled Fusion*, vol. 61, no. 1, p. 014035, 2018.
- [3] N. Riva, R. S. Granetz, R. Vieira, A. Hubbard, A. T. Pfeiffer, P. Harris, C. Chamberlain, Z. S. Hartwig, A. Watterson, D. Anderson, and R. Volberg, "Development of the first non-planar rebco stellarator coil using viper cable," *Superconductor Science and Technology*, vol. 36, no. 10, p. 105001, aug 2023. [Online]. Available: <https://dx.doi.org/10.1088/1361-6668/aced9d>
- [4] D. A. Gates, D. Anderson, S. Anderson, M. Zarnstorff, H. Weitzner, D. Ruzic, D. Andruczyk, A. Reiman, J. D. Lore, M. Landreman, J. P. Freidberg, S. R. Hudson, M. Porkolab, D. Demers, J. Terry, E. Edlund, S. A. Lazerson, N. Pablant, R. Fonck, F. Volpe, J. Canik, R. Granetz, A. Ware, J. D. Hanson, S. Kumar, C. Deng, K. Likin, A. Cerfon, A. Ram, A. Hassam, S. Prager, C. Paz-Soldan, M. J. Pueschel, I. Joseph, and A. H. Glasser, *Stellarator Research Opportunities: A Report of the National Stellarator Coordinating Committee*. Springer US, 2018, vol. 37, no. 1.
- [5] A. H. Boozer, "Why carbon dioxide makes stellarators so important," *Nuclear Fusion*, vol. 60, no. 6, 2020.
- [6] D. Gates, A. Boozer, T. Brown, J. Breslau, D. Curreli, M. Landreman, S. Lazerson, J. Lore, H. Mynick, G. Neilson, N. Pomphrey, P. Xanthopoulos, and A. Zolfaghari, "Recent advances in stellarator optimization," *Nuclear Fusion*, vol. 57, no. 12, p. 126064, oct 2017. [Online]. Available: <https://dx.doi.org/10.1088/1741-4326/aa8ba0>
- [7] C. Beidler, E. Harmeyer, F. Herrnegger, Y. Igitkhanov, A. Kendl, J. Kisslinger, Y. Kolesnichenko, V. Lutsenko, C. Nührenberg, I. Sidorenko, E. Strumberger, H. Wobig, and Y. Yakovenko, "The helias reactor hsr4/18," *Nuclear Fusion*, vol. 41, no. 12, p. 1759, dec 2001. [Online]. Available: <https://dx.doi.org/10.1088/0029-5515/41/12/303>
- [8] T. Andreeva, C. D. Beidler, E. Harmeyer, Y. L. Igitkhanov, Y. I. Kolesnichenko, V. V. Lutsenko, A. Shishkin, F. Herrnegger, J. Kißlinger, and H. F. G. Wobig, "The helias reactor concept: Comparative analysis of different field period configurations," *Fusion Science and Technology*, vol. 46, no. 2, pp. 395–400, 2004.
- [9] N. Riva, A. Halbach, M. Lyly, C. Messe, J. Ruuskanen, and V. Lahtinen, " H - ϕ formulation in sparselizard combined with domain decomposition methods for modeling superconducting tapes, stacks, and twisted wires," *IEEE Transactions on Applied Superconductivity*, vol. 33, no. 5, pp. 1–5, 2023.
- [10] C. R. Vargas-Llanos, F. Huber, N. Riva, M. Zhang, and F. Grilli, "3d homogenization of the t-a formulation for the analysis of coils with complex geometries," *Superconductor Science and Technology*, vol. 35, no. 12, p. 124001, oct 2022.
- [11] A. Bossavit, "Whitney forms: A class of finite elements for three-dimensional computations in electromagnetism," *IEE Proceedings A (Physical Science, Measurement and Instrumentation, Management and Education, Reviews)*, vol. 135, no. 8, pp. 493–500, 1988.
- [12] H. Schwarz, "Ueber einige abbildungsaufgaben." vol. 1869, no. 70, pp. 105–120, 1869. [Online]. Available: <https://doi.org/10.1515/crll.1869.70.105>
- [13] P.-L. Lions et al., "On the schwarz alternating method. i," in *First international symposium on domain decomposition methods for partial differential equations*, vol. 1. Paris, France, 1988, pp. 1–42.
- [14] Z. S. Hartwig, R. Vieira, B. N. Sorbom, R. A. Badcock, M. Bajko, W. K. Beck, B. Castaldo, C. L. Craighill, M. Davies, J. Estrada, V. Fry, T. Golfopoulos, A. E. Hubbard, J. H. Irby, S. Kuznetsov, C. J. Lammi, P. Michael, T. Mouratidis, R. A. Murray, A. T. Pfeiffer, S. Z. Pierson, A. Radovinsky, M. D. Rowell, E. E. Salazar, M. Segal, P. W. Stahle, M. Takayasu, T. L. Toland, and L. Zhou, "VIPER: An industrially scalable high-current high temperature superconductor cable," *Superconductor Science and Technology*, no. 33, p. 11LT01, 2020.
- [15] Z. Zhao, P. Moore, and L. Chiesa, "Structural modeling of rebco viper cable for high-field magnet applications," *IEEE Transactions on Applied Superconductivity*, vol. 32, no. 6, pp. 1–5, 2022.
- [16] —, "Structural finite element analysis of rebco tape delamination with solid-shell element under various loads," *IOP Conference Series: Materials Science and Engineering*, vol. 1241, no. 1, p. 012032, may 2022.
- [17] F. Pierro, Z. Zhao, L. Chiesa, G. Celentano, M. Marchetti, and A. della Corte, "Structural modeling of hts cable-in-conduit conductor with helically slotted aluminum core for high-field magnet applications," *IEEE Transactions on Applied Superconductivity*, vol. 30, no. 4, pp. 1–5, 2020.
- [18] "COMSOL Multiphysics® v. 6.0. (Website), COMSOL AB, Stockholm, Sweden." [Online]. Available: www.comsol.com
- [19] K. O. Lye, S. Mishra, and R. Molinaro, "A multi-level procedure for enhancing accuracy of machine learning algorithms," *European Journal of Applied Mathematics*, vol. 32, no. 3, pp. 436–469, 2021.